

Effect of Ball Milling Process on the Characteristics of Natural Based- And Synthetic Based-Wollastonite for Biomedical Application

Nur Hasnidah Ahmad Shukeri^{1*} and Syed Nuzul Fadzli Bin Syed Adam¹

¹ Faculty of Mechanical Engineering & Technology, Universiti Malaysia Perlis, Perlis, Malaysia.

Received 30 April 2024, Revised 3 June 2024, Accepted 6 June 2024

ABSTRACT

Wollastonite (CaSiO_3) is a potential biomaterial, particularly beneficial for biomedical purposes such as tissue bone regeneration. The objective of this study is to evaluate the effect of dry and wet milling conditions on the formation of solid wollastonite bioceramic. In this study, synthetic-type wollastonite was produced from chemically synthetic powder; meanwhile, a combination of seashells and rice husk ash (RHA) was used to form natural-type wollastonite. In sample preparation, CaO and SiO_2 powder (1:1 weight ratio) were milled together by planetary ball milling operation under different milling conditions: dry and wet milling. The ball-milled powder mixtures were compacted before sintering at 1200°C for 4 hours. The weight loss and shrinkage of the samples were measured and characterized using XRD, FTIR, and SEM analysis. The results confirmed that the wollastonite phase was formed after the sintering process for both dry and wet ball milled processes with anorthic and monoclinic structure types of calcium silicate phases. The wet-milled processed natural powders relatively formed denser bodies and had a higher weight loss percentage compared to dry-milled processed synthetic powders. In conclusion, wet milling is a more suitable method for producing solid wollastonite via powder sintering. In addition, the natural-based sources from RHA and seashells were able to reach the mineralogical properties comparable to synthetic-based sources for forming wollastonite, which could be promising as an alternative material in biomedical applications.

Keywords: Dry and wet ball milling, Natural and synthetic-derived sources, Rice husk ash (RHA), Seashells, Wollastonite.

1. INTRODUCTION

Wollastonite, CaSiO_3 is a calcium silicate ceramic formed by a combination of calcium oxide, CaO , and silica dioxide, SiO_2 compounds with a chemical composition of 48.25% and 51.75%, respectively [1]. It has great mechanical properties such as high thermal resistance and stability in chemical structure as well as non-toxicity and corrosion resistance, which promotes its application in various industries such as ceramic, plastic, and coating [2]. Some studies have verified that wollastonite could be commercially used, particularly for biomedical purposes, as it is a bioactivity and biocompatibility material, which is appropriate for bone tissue regeneration and teeth repair and replacement [1], [3], [4]. Generally, wollastonite can be classified into two types of polymorphic forms, which are pseudo-wollastonite ($\alpha\text{-CaSiO}_3$) and beta-wollastonite ($\beta\text{-CaSiO}_3$). A study [4] has stated that the $\alpha\text{-CaSiO}_3$ with triclinic lattice structure can be formed at high temperatures, which is within $1125\text{-}1436^\circ\text{C}$. Meanwhile, the $\beta\text{-CaSiO}_3$ has long single-chain silicate crystallization, formed at low temperature, which is not over 1125°C .

*Corresponding author: nurhasnidah@studentmail.unimap.edu.my

Over the past years, the wollastonite has been produced by many researchers by using synthetic-based sources. A study [5] has performed an investigation on the production of CaSiO_3 ceramics for high load-bearing applications for biomedical purposes. They recorded that the synthesization of calcium silicate powder was associated with the addition of 5 wt. % of silica sol via precipitation process and sintered at 1100°C has produced 186.2 MPa flexural strength and 3.9% open porosity. Besides, synthetic wollastonite can also be produced by the mixtures of heat-treated borogypsum and potassium hydroxide in a stoichiometric ratio. It was sintered at the range of $900\text{-}1000^\circ\text{C}$ for an hour [6]. They mentioned that synthesizing borogypsum with additive materials could achieve the wollastonite samples with increasing strength and reducing water absorption.

However, at present, the production of wollastonite has been explored by using natural-based sources due to high demand in a wide range of industries. Instead of using synthetic-derived sources for the production of wollastonite, natural-derived sources were exploited as alternative sources to substitute for synthetic sources. Plenty of researchers have done reviews and analyses using a combination of natural waste such as paddy straw, rice husk ash (RHA), eggshells, seashells, and others for wollastonite production. The usage of these materials not only could lessen the cost expenditure and make it more convenient and reachable for continuous supply but also maintain the sustainability of the development of non-renewable sources such as limestone and silica sand. Thus, producing wollastonite substances would involve a ball milling operation to mix the initial materials homogeneously, which can be performed either dry or wet ball milling and subsequently furthered with the sintering process.

Generally, the ball milling process can be processed with two conditions of the ball mill, which are dry and wet ball milling. The dry ball milled operation would cause agglomeration of the mixed powders [7] and reduce its mechanical properties. Besides, the dry ball milled could also cause contamination of unnecessary elements in the mixed powders due to the friction generated between the raw powder, ball mediums, and wall of the milling jar. The limitations of previous research on wet milling powders to produce wollastonite have also encouraged the implementation of the experiment in this study. Hence, the aim of this study is to investigate the effect of dry and wet ball milling process; and the use of natural-derived and synthetic-derived powders on the formation and properties of solid wollastonite. It is crucial to determine which milling processes are more suitable for producing solid wollastonite and the potential of alternative natural resources in wollastonite production.

In this study, seashells and rice husk ash (RHA) were used as natural sources as they could provide sustainable development at a lower cost compared to synthetic sources. An investigation of natural-derived and synthetic-derived powders using the dry and wet ball milling process will be carried out. The significance of this study lies in the utilization of natural sources, as this study was looking forward to using these wastes as an alternative material to substitute the synthetic sources in the production of wollastonite, particularly for bone tissue regeneration applications. The weight loss and shrinkage of the samples were measured, and several tests and characterizations will be performed to study the effect of natural-derived and synthetic-derived powders by dry and wet ball milling processes on the properties of the produced wollastonite. X-ray diffraction (XRD), Fourier-transform infrared spectroscopy (FTIR), and Scanning Electron Microscopy (SEM) were analyzed to observe the structural analysis and surface morphology of the samples.

2. MATERIAL AND METHODS

In this study, synthetic and natural-based materials were used to determine the compatibility of both material resources in producing wollastonite (CaSiO_3). Synthetic CaOH and SiO_2 powders were used as the standard synthetic-based material in this study. On the other hand, natural-

based materials were also utilized to produce CaSiO_3 , where the seashells were collected from the local beach drift while the rice husk was obtained from the waste of paddy agricultural industries. These materials were heat treated separately to compose the CaO and SiO_2 elements for the purpose of creating the reactions between both elements for the production of CaSiO_3 during the sintering process. Plus, ethanol was used as a solvent medium during the wet ball milling operation as it was expected to enhance the milling performance homogeneously and reduce the agglomeration of milled powders.

2.1 Preparation of Raw Materials

The seashells were rinsed with ethanol and water and then dried at $120\text{ }^\circ\text{C}$ for 4 hours in a hot air universal oven (Memmert UN55 Plus). The porous seashells were crushed and sieved to obtain small pieces of granular seashells. It was preceded by a ball milling operation with a milling speed of 400 rpm for an hour. The seashell powders were heated at $1100\text{ }^\circ\text{C}$ for 4 hours with $5\text{ }^\circ\text{C}/\text{min}$ in the furnace (LT Furnace SIC4-1600) to obtain the CaO elements.

The rice husks were dried at $80\text{ }^\circ\text{C}$ for a day in the oven to get rid of the presence of moisture in the material. Then, it was heated in the furnace at $1100\text{ }^\circ\text{C}$ for 4 hours to decarbonize the material and achieve the SiO_2 elements. The rice husk ashes (RHA) were sieved to filter and collect the fine particles of powders.

2.2 Ball Milling Operation

The synthetic-based CaOH and SiO_2 powders were milled together by using a planetary milling machine (Mono Mill Pulverisette 6-classic line, Fritsch, Germany) with 50 numbers of 5 mm diameters of agate grinding balls with 250 mL agate milling jar (Fritsch, Germany). The synthetic-based powders were dry milled together at 450 rpm for 2 hours with the ratio of CaOH and SiO_2 powders was 1:1. The ball milled operation was repeated for the production of wet milled samples of CaSiO_3 with an addition of 40 mL of ethanol as the milling medium. For the wet ball milled powders, the milled powders of CaOH and SiO_2 were dried in the oven at 110°C overnight for the purpose of achieving completely dry powder mixtures by eliminating the moisture in the mixed powders. Then, the dried powders were fined with a pestle and mortar to create small powder particles. Both conditions of the ball milling operation (dry and wet ball milling) were repeated by using natural-based materials with the heated seashells and RHA that had been prepared previously. The methods applied by the natural-based sources were similar to those implemented by the synthetic-based sources.

2.3 Wollastonite Production

The 2g of milled powders were inserted into a high carbon steel mold to create a compact small disc of pellets with 20 mm diameter and 4 mm thickness for each pellet. The milled powders were compacted with a hydraulic press machine (Nichi T-61230A) under 33 MPa of loads with a holding time of 5 minutes. The pellets were sintered in the furnace (LT Furnace SIC4-1600) at 1200°C for 4 hours with a cooling rate of $3^\circ\text{C}/\text{min}$.

2.4 Sample Characteristics

The raw powders of natural and synthetic sources were tested by using X-ray diffraction (XRD machine, Test Instrument Bruker, D2 Phaser Germany 2010) with angle diffraction of the testing applied at the range of 10° to 80° (2θ) of step-scanning for 10 minutes of loading time for each sample. This testing was made to examine the crystallinity and phase transformation that exists in the raw powder. Analyses of the raw material were made to determine the presence of CaO and SiO_2 elements. Besides, the samples of sintered pellets were also tested to verify the formation of CaSiO_3 in the samples. The data of the tested samples were analyzed by

using Highscore Plus software to identify the phases that match with the standard databases then plotted with Origin Lab software.

The raw powders and sintered pellets of natural and synthetic-based sources with both conditions of ball milling, which is dry and wet ball milling processes, were tested with Fourier transform infrared spectroscopy (FTIR, Perkin Elmer, USA) to detect the presence of infrared spectrum in the samples. The samples were prepared individually by mixing the sample powders with potassium bromide KBr powder with a ratio of 1:10. The mixed powders were compacted under 5 tons of loads and dried in a vacuum oven to seal the samples before the FTIR testing.

Scanning electron microscopy (SEM) of Philips XL30 ESEM was used during SEM testing for the samples of synthetic and natural sources of raw material powders and sintered pellets. The samples were coated with a thin layer of gold (Au) by the sputter coating (Quorum Q150R) to prevent charging during the testing and obtain high-quality images of the samples. The magnification used to observe the surface morphology of the samples was around 1000X, 3000X, and 5000X for the purpose of identifying the characteristics of the surface structure of the samples. The images obtained were analyzed using Image J software to indicate the porosity of the samples. Besides, the samples are also associated with Energy Dispersive X-Ray Analysis (EDX) analysis to determine the quantity of the elements that may exist in the samples.

The weights of the sintered pellets were recorded before and after the milling and sintering process to calculate the weight loss of the samples. The samples were weighted thrice to obtain the average of each sample. The data recorded were calculated by using Equation 1 to obtain the weight loss percentage of the samples.

$$\text{Weight loss (\%)} = \frac{(w_1 - w_0)}{w_0} \times 100 \quad (1)$$

Noted that;

w_1 = Final weight of the samples after the sintering process

w_0 = Initial weight of the samples before the sintering process

The diameter and thickness dimensions of each sintered pellet were measured before and after the sintering operation in order to indicate the shrinkage of the samples. The samples were measured thrice using a vernier caliper to achieve an accurate reading of the dimensional, and the average readings were taken to calculate the volume of the pellets. Then, the shrinkage percentages were calculated by using Equations 2 and 3.

$$\text{Volume shrinkage (\%)} = \frac{(V_1 - V_0)}{V_0} \times 100 \quad (2)$$

$$\text{Volume, } V = \pi \left(\frac{d}{2}\right)^2 h \quad (3)$$

Noted that;

V_1 = Final volume of the sample after the sintering process

V_0 = Initial volume of the sample before the sintering process

d = Diameter of the sample

h = Thickness of the sample

3. RESULTS AND DISCUSSION

3.1 Weight Loss

The illustration from Figure 1 demonstrates the weight loss percentage of dry and wet ball mills produced by natural-derived and synthetic-derived powders. It shows that the weight loss percentage of synthetic dry ball milled (13%) is higher than that of natural dry ball milled (6%). This is probably because the pure elements of raw synthetic dry ball milled powders react after the sintering process and lead to the elimination of unnecessary substances such as hydrogen or carbon ions. Meanwhile, the percentage of weight loss of natural-derived powder by wet ball milled operation (17.5%) is slightly higher than the synthetic wet ball milled sample (16%), where the weight loss may happen due to the usage of ethanol as solvent where it dissolves more volatile substances that may contents in the mixed powders of the natural-derived during wet ball milling.

Moreover, Figure 1 also shows that the wet ball milled produced from natural-derived powder (17.5%) is higher than the dry ball milled from natural-derived powder (6%). Meanwhile, the synthetic-derived, wet ball milled powders (16%) are higher than the synthetic-derived, dry ball milled powders (13%). These findings proved that the wet ball milled operation creates larger weight loss compared to dry ball milled operation either from natural-derived or synthetic-derived powder. This is because the ethanol used in wet ball milled as lubrication promotes the equivalent milling of powders and produces extremely fine particles of powders. Furthermore, the dry ball milled operation shows less weight loss reduction due to the creation of distinguishable agglomeration and the production of uneven particles, as shown in Figure 2.

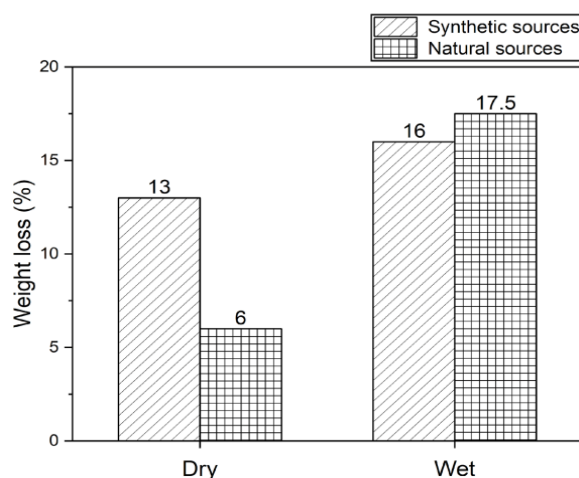


Figure 1: Bar chart of percentage of weight loss of dry and wet balls milled from natural-derived and synthetic-derived powders.

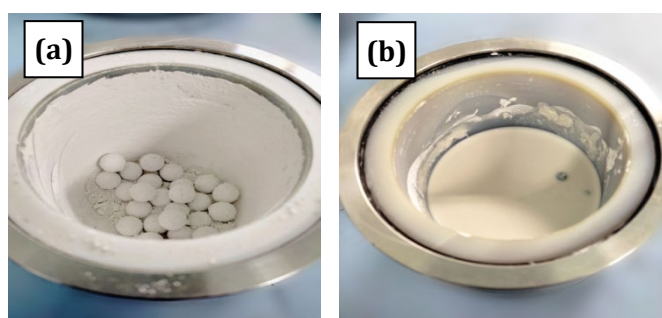


Figure 2: (a) Dry and (b) wet ball milled powder after the milling process.

3.2 Shrinkage

Figures 3 and 4 show the prominent contrast in shrinkage of dry milled and wet milled from natural-derived powders. The highest shrinkage can be observed in natural-derived wet ball milled operation (41.7%), while the least shrinkage is attained by the synthetic-derived wet ball milled (1.41%). The high shrinkage from the natural derived-wet ball milled could be because of extremely fine particle powders created and caused the excessive compaction and vigorous grain growth in the samples. On the other hand, the least shrinkage from the synthetically derived wet ball milled may be due to the inactive grain growth of the sample during the sintering process. Overall, the dry milled operation from natural-derived and synthetic-derived sources create 8.74% and 2.91%, respectively. It also clarified that the synthetic-derived powder, dry milled (8.74%), is higher than wet milled (1.41%). Meanwhile, the natural-derived powder with dry milled (2.91%) is excessively lower than wet milled (41.7%) because it is assumed that the wet milling operation provides homogenous milling and produces fine particle powders that promote high densification. These could also be due to the discarded elements from the sample pellets after the sintering process, such as hydrogen and carbon elements, which supports the weight loss findings.

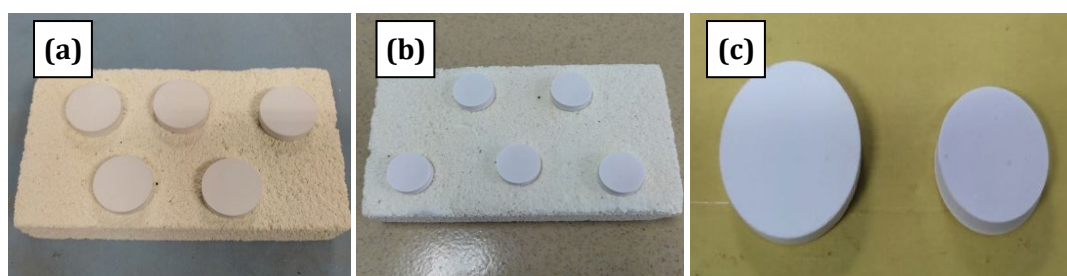


Figure 3: The sample pellets of (a) dry ball milled (b) wet ball milled and (c) difference between dry and wet ball milled.

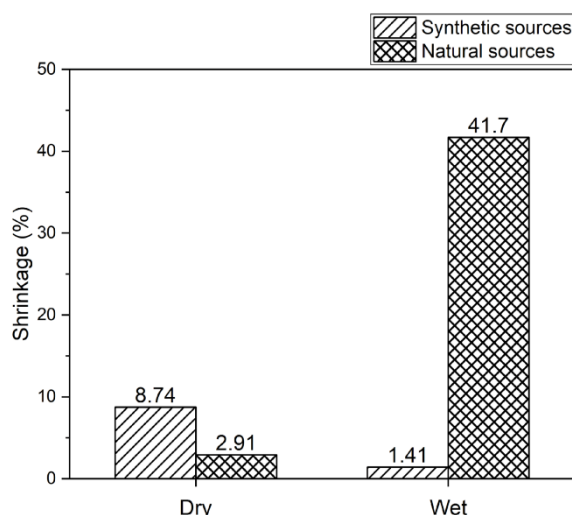


Figure 4: Bar chart of shrinkage of dry and wet ball milled from natural-derived and synthetic-derived powders.

3.3 Phase Transformation Analysis

According to the diffractogram shown in Figure 5, it shows the XRD patterns of heated seashells and synthetic-based powders, which consist of CaO and CaOH simultaneously. The cubic (JCPDS

file no. 00-070-5490) and hexagonal (JCPDS file no. 00-004-0733) types were found in the heated seashell samples. Several studies [8], [9] also have shown a similar XRD pattern of heated seashells as obtained in this study. Nevertheless, it was found that the present study obtained cubic type (JCPDS file no. 00-033-0664) at the diffraction angle peaks of 38.12° , 44.28° , 64.47° , 77.73° and 80.10° . The higher intensity of peaks in the diffractogram of heated seashells demonstrated that it has higher diffracted planes that contain a greater amount of atoms, which actively create large numbers of electrons during XRD testing compared to synthetic-derived powder. Meanwhile, the synthetic-derived powders also have the same crystal system with different phases, which are hexagonal (JCPDS file no. 00-002-0969 and JCPDS file no. 01-084-1265).

The diffractogram of heated RHA and chemically synthetic-based powder is presented in Figure 6. It shows that both sample powders had SiO_2 elements yet with different crystal systems. The heated RHA had orthorhombic (JCPDS file no. 00-045-1401) and tetragonal (JCPDS file no. 00-011-0695) types, while hexagonal (JCPDS file no. 01-070-3755) and tetragonal (JCPDS file no. 01-080-3753) types were found in synthetic-derived sample powders. The RHA sample was assumed to have a slightly amorphous phase similar to that stated in a previous study [10], [11] because of a broad angle diffraction from 19.95° to 24.94° . In contrast with the RHA sample, the synthetic-derived powder shows a complete crystallite phase due to the observed sharp and narrow peaks in the diffractogram.

Figure 7 illustrates the diffractogram of the synthetic-based and natural-based wollastonite processed by dry and wet ball milling operations. They present the existence of calcium silicate ceramic elements that were created and confirm that the formation of wollastonite has been successfully produced. These samples consist of obvious peaks at similar diffraction angles, which are at 26.00° , 31.90° , 36.70° , 45.43° and 45.88° . The samples involve anorthic type (JCPDS file no. 01-074-0874) and monoclinic type (JCPDS file no. 01-080-9543 and JCPDS file no. 01-089-6463). All the wollastonite formed can be considered fully crystallite due to the sharp peak diffractions. At the diffraction peak of 45.88° , the anorthic type existed in every sample of wollastonite either made by natural-based or synthetic-based sources with dry or wet ball mill operation. Meanwhile, at the highest intensity of each diffractogram, which is at a peak of around 27.66° , the monoclinic type was found in every wollastonite sample except samples of synthetic-based produced by dry ball mill operation.

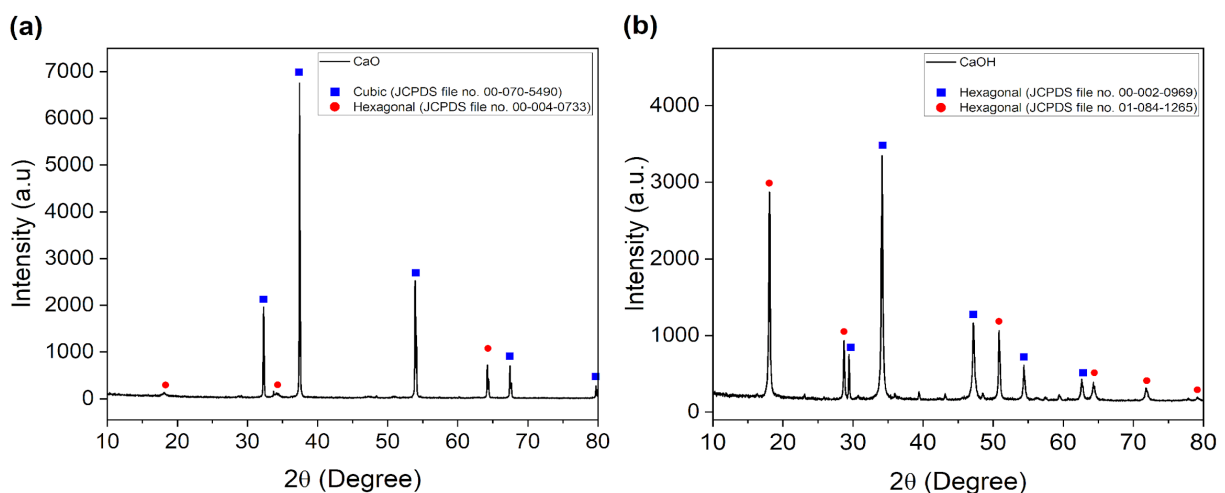


Figure 5: Diffractogram of (a) heated seashells (b) synthetic-based CaOH powder.

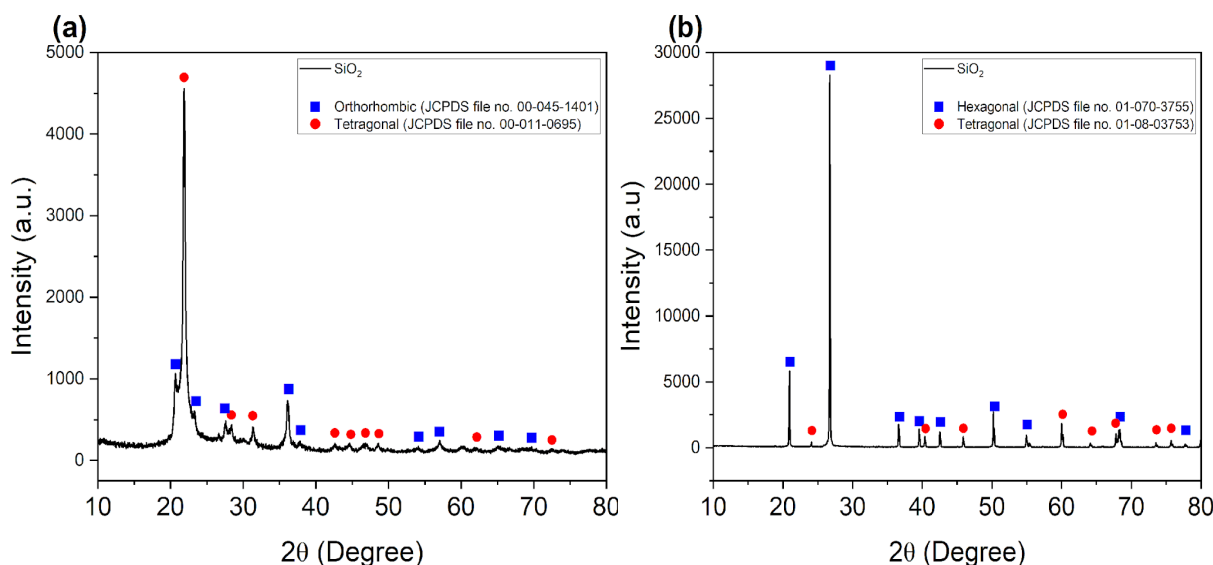


Figure 6: Diffractogram of (a) heated RHA (b) synthetic-based SiO_2 powder.

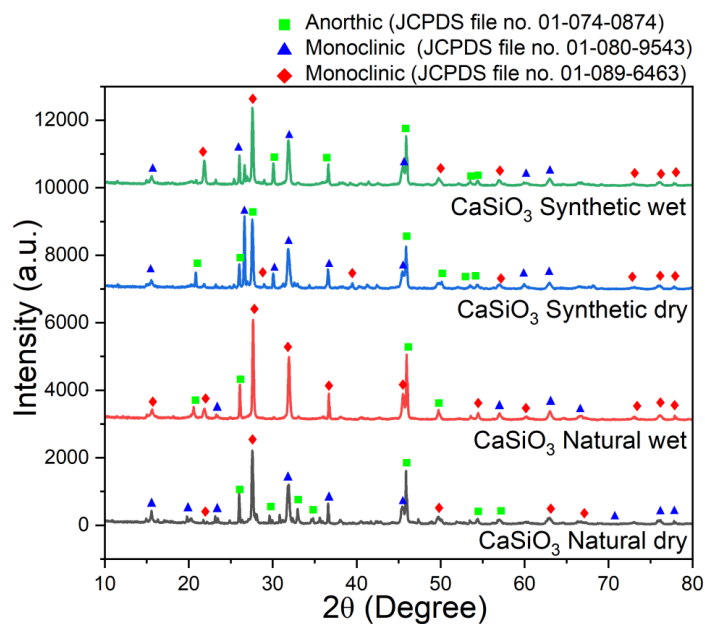


Figure 7: Diffractogram of synthetic-based and natural-based of dry and wet ball milled wollastonite.

3.4 Infrared Spectrum Analysis

Figure 8 (a) shows FTIR analysis of milled seashells and heated seashells. The heated seashells consist of a bending bond of C-O between the atoms of oxygen and calcium in carbonates [12] at a centered wide band of 1474 cm^{-1} , smaller than the band of milled seashells. The C-O bond is also found at 2520 and 2920 cm^{-1} bands in the milled seashell samples but not in the heated seashell samples. It can be assumed that it is due to the bond that has been broken, which eliminated the carbonate ions after the sintering process. The tiny bands that existed at 717 , 870 and 1790 cm^{-1} were due to the stretching mode of C-O, possibly because of the production of CO_2 in the environment during the heating process [12]. Next, Ca-O bending modes were assigned at the band of 558 cm^{-1} . An O-H stretching bond at 3645 cm^{-1} band is due to the moisture condition on the surface of the samples.

The heated RHA was analyzed with FTIR testing, which has been shown in Figure 8 (b). Generally, the FTIR analysis obtained in the experiment was nearly identical to previous research [13], [14]. At 490 and 623 cm^{-1} bands, a Si-O stretching bond was assigned, claiming the silica elements exist in the RHA samples. Moreover, there was also Si-O-Si bending mode at a centered wider band of 1114 cm^{-1} , O-H bending mode at a tiny band of 1622 cm^{-1} , and C-H stretching bond at 2920 cm^{-1} . An asymmetry band at 3442 cm^{-1} appeared as O-H bonding, similar to a previous study [13].

Based on Figure 9, it resembles the FTIR of wollastonite formed with natural-based and synthetic-based produced by dry and wet ball milling operations. It shows that the fluctuation spectrum of all samples was almost similar to each other even though different based-powder sources and ball milling mediums controlled the factors. However, there is an obvious contradiction of fluctuation for CaSiO_3 synthetic dry samples at the early peak, specifically at less than 500 cm^{-1} compared to other wollastonite samples. The broad peaks at 3200 to 3659 cm^{-1} range were due to the O-H bending modes, while the peak of 1630 cm^{-1} represents a weak stretching OH mode, which concurs with a study [15]. There is also a Si-O-Si stretching bond at the band around 563, 658, and 963 cm^{-1} while stretching the O-Si-O bond at 797 cm^{-1} . The peak of 1417 cm^{-1} resembles the bending mode of carbonate ions or CO_2 generated during the sintering process [16].

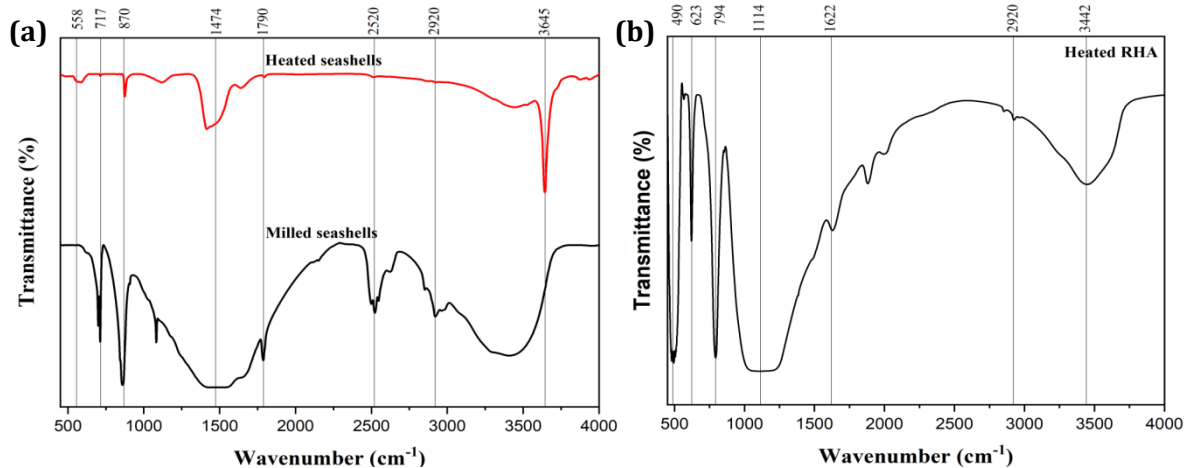


Figure 8: FTIR analysis of (a) heated and milled seashells, and (b) heated RHA.

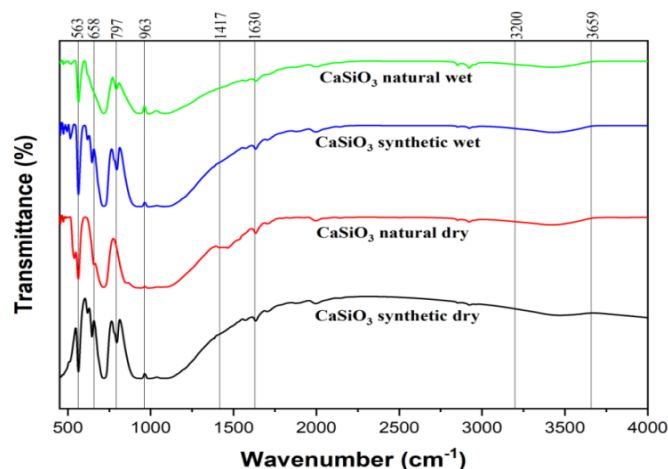


Figure 9: FTIR analysis of wollastonite-derived from synthetic and natural sources with dry and wet ball milling.

3.5 Surface Morphology

Figure 10 illustrates the SEM of heated seashells and synthetic-based CaOH powder. It is assumed that the bright white part in the morphology is due to the diffracted electrons that promote to emit them during the testing and verified the presence of calcium elements in the samples. The heated seashells show tiny and flaky structures [9] of aggregate, while the CaOH synthetic-based powders present nanoparticle powder [8] with irregular particle sizes.

Figure 11 presents the surface morphology of heated RHA and SiO₂ synthetic-derived powder. The observed morphology shows that the RHA seems like a continuous cellulose fiber with uneven surface roughness, possibly due to the impurities in the substances adhered to RHA samples [17] and some tiny pores on the sample [18]. Meanwhile, the SiO₂ synthetic powder shows irregular, sharp edges of granular shapes with particles of uneven size.

Next, Figure 12 shows the structural analysis by SEM at 3000X magnification on the natural-derived wollastonite processed by dry and wet ball milling. Both natural-derived wollastonite samples, either dry or wet ball mill showed irregular granular shapes of particles in the morphology. It is extremely obvious and noticeable that wet milled wollastonite is less dense than dry milled wollastonite. This is because it has an active grain growth reaction in the wet ball milled sample since the used ethanol acts as the solvent, providing a homogenous milling performance and producing fine particle powders. The wet milled wollastonite also showed higher porosity (4.90%) than dry milled wollastonite as the elements by the ethanol would decompose during the sintering process and leave plenty of small voids in the sample and, in resulting the arrangement of particles is seen more porous. This is similar to a study where the mineralizer used B₂O₃ formed a slight amount of pores with excessive large grain growth [19].

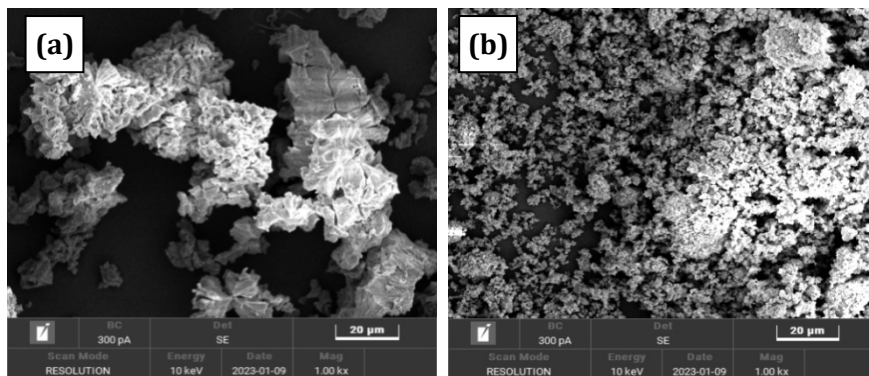


Figure 10: SEM of (a) heated seashells (b) synthetic-derived CaOH powder at 1000X magnification.

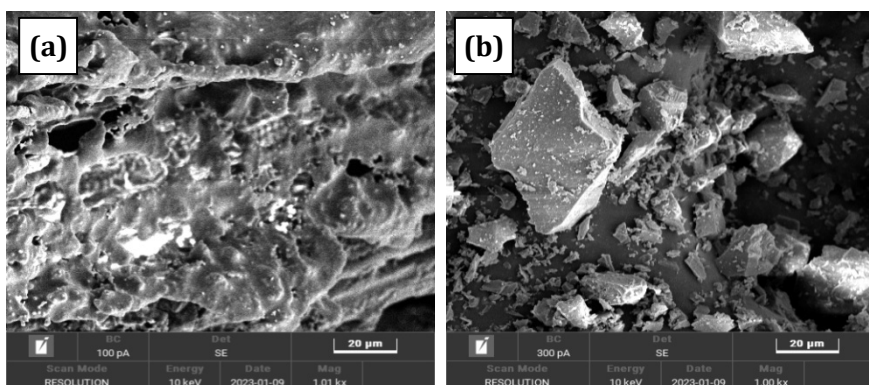


Figure 11: SEM of (a) heated RHA (b) synthetic-derived SiO₂ powder at 1000X magnification.

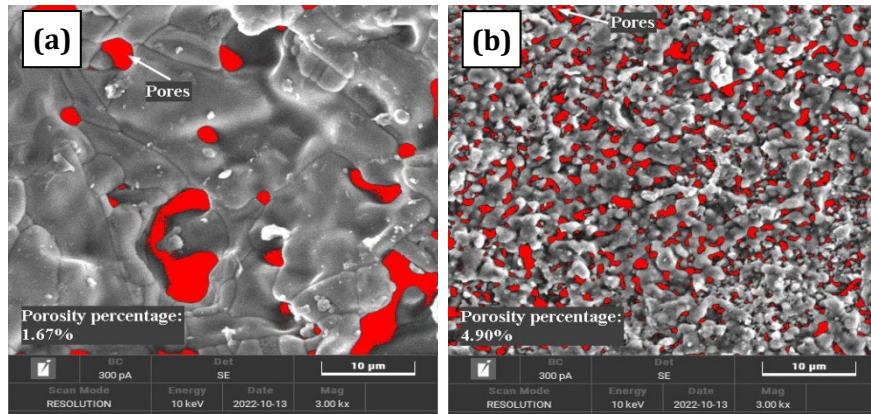
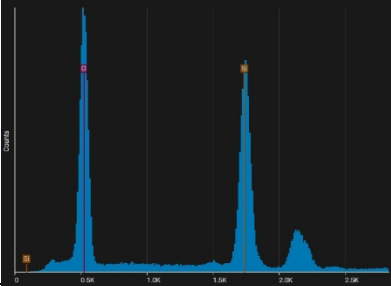
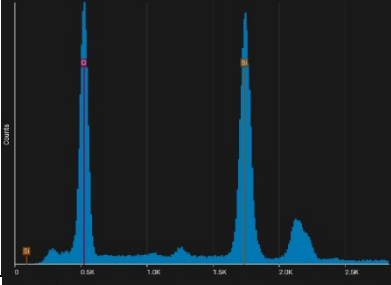
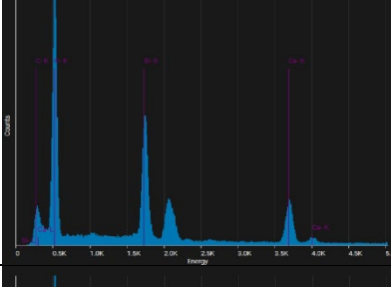
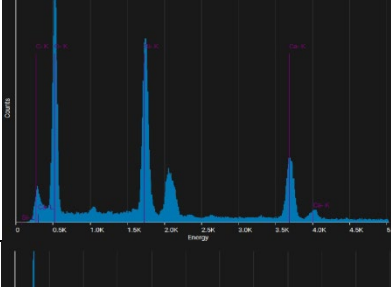




Figure 12: SEM of natural-derived wollastonite by (a) dry and (b) wet ball mill operation.

Moreover, the images scanned by SEM were used to perform EDX analysis, which was presented in Table 1, where the quantity analyses of the elements were recorded in the samples. These recorded data by EDX have shown that the presence of elements in the samples indirectly emphasized and supported the previous findings obtained by XRD and FTIR. However, the element of carbons has been identified in the heated seashells at about 13.69%, which could be assumed that the temperature applied during the heat treatment on this initial material is not sufficient enough to eliminate the entire carbonate contents, meanwhile, the carbon elements in the synthetic powder of CaOH could be due to the frequent exposure with the surrounding and leads to the reaction with the CO₂ in the environment. These carbon contents have subsequently influenced the contents of wollastonite samples too, either in dry-milled or wet-milled powders. Regardless of the carbon contents from the initial materials, it can be seen that respectively both synthetic and natural derived of the wet-mill powders (19.25% and 30.85%) have higher carbon contents compared to the dry-milled powders (15.58% and 13.02%), which may be due to a residue from the usage of ethanol after the sintering process.

Table 1: EDX analysis on the dry and wet ball milled from synthetic and natural-derived wollastonite.

Samples	Weight (%) of the Elements				Spectrum
	Ca	O	C	Si	
CaOH powders	47.63	31.83	20.55	-	
Seashells	55.18	31.13	13.69	-	

SiO₂ powders	-	54.57	-	45.43	
RHA	-	50.68	-	49.32	
Dry milled, synthetic-derived	20.57	40.12	15.58	23.73	
Wet milled, synthetic-derived	28.34	34.31	19.25	18.10	
Dry milled, natural-derived	20.07	34.20	13.02	32.71	
Wet milled, natural-derived	14.08	39.15	30.85	15.92	

4. CONCLUSION

The objectives of this study were successfully achieved. In this study, it can be concluded that seashells and rice husks can be used to produce wollastonite compounds that are comparable to chemically synthetic-derived powders. Both factors, which are synthetic and natural-derived powders, together with dry and wet milling operations, are still able to form wollastonite phases. However, the wet milling process is a more suitable method for producing solid wollastonite due to its better handling process, as no agglomeration happens and instead promotes the homogeneity of powder mixing. Besides, the wollastonite from natural-derived also has proven physical and morphological characteristics appropriate for bone tissue regeneration application. Thus, it can be expected that the mechanical properties of this wet milled wollastonite are higher compared to dry milled wollastonite with great bioactivity performances. Since natural-based wollastonite was found to be comparable to synthetic-based wollastonite, the usage of natural sources should be studied further due to the non-toxicity and organic materials, low cost of expenses, convenience for continuous supply as well as the sustainability of waste development by the abundance of natural sources.

ACKNOWLEDGEMENTS

A deep gratitude is also expressed to the Faculty of Mechanical Engineering & Technology of Universiti Malaysia Perlis (UniMAP) for providing the facilities of labs, machines and equipment and allowing for the experiment and testing works to be implemented.

REFERENCES

- [1] Zakaria, M. Y., Sulong, A. B., Muhamad, N., Raza, M. R., & Ramli, M. I. Incorporation of wollastonite bioactive ceramic with titanium for medical applications: An overview. *Materials Science and Engineering: C*, vol 97, (2019) pp. 884-895.
- [2] Zhou, R., Wang, J., Wang, X., Zhang, H., Sun, S., Li, Y., ... & Liang, Y. Superhydrophilic wollastonite-nanoTiO₂ composite photocatalyst prepared by a wet grinding method: The effects of carriers and their application in the self-cleaning coatings. *Ceramics International*, vol 48, issue 10 (2022) pp. 13770-13779.
- [3] Palakurthy, S., & Samudrala, R. K. In vitro bioactivity and degradation behaviour of β -wollastonite derived from natural waste. *Materials Science and Engineering: C*, vol 98, (2019) pp. 109-117.
- [4] Ismail, H., & Mohamad, H. Bioactivity and biocompatibility properties of sustainable wollastonite bioceramics from rice husk ash/rice straw ash: A review. *Materials*, vol 14, issue 18 (2021) p. 5193.
- [5] Pan, Y., Yin, J., Yao, D., Zuo, K., Xia, Y., Liang, H., & Zeng, Y. Effects of silica sol on the microstructure and mechanical properties of CaSiO₃ bioceramics. *Materials Science and Engineering: C*, vol 64, (2016) pp. 336-340.
- [6] Yarusova, S. B., Gordienko, P. S., Buravlev, I. Y., Kozin, A. V., Zhevtun, I. G., & Okhlopkova, A. A. Production of Synthetic Wollastonite Using Gypsum Technogenic Raw Materials. *KnE Materials Science*, (2020) pp. 511-524.
- [7] Eze, A. A., Sadiku, E. R., Kupolati, W. K., Snyman, J., Ndambuki, J. M., Jamiru, T., ... & Desai, D. A. Wet ball milling of niobium by using ethanol, determination of the crystallite size and microstructures. *Scientific reports*, vol 11, issue 1 (2021) p. 22422.
- [8] Alobaidi, Y. M., Ali, M. M., & Mohammed, A. M. Synthesis of Calcium Oxide Nanoparticles from Waste Eggshell by Thermal Decomposition and their Applications. *Jordan Journal of Biological Sciences*, vol 15, issue 2 (2022).
- [9] Singh, T. S., & Verma, T. N. Analysis of the effect of temperature on the morphology of egg shell calcium oxide catalyst: Catalyst production for biodiesel preparation. *Scientia*

- Iranica, vol 27, issue 6 (2020) pp. 2915-2923.
- [10] Silva, D., Pachla, E., Marangon, E., Tier, M., & Garcia, A. P. Effects of rice husk ash and wollastonite incorporation on the physical and thermal properties of refractory ceramic composites. *Matéria* (Rio de Janeiro), vol 25, (2020) p. e-12802.
- [11] Sompech, S., Dasri, T., & Thaomola, S. Preparation and characterization of amorphous silica and calcium oxide from agricultural wastes. *Orient. J. Chem*, vol 32, issue 4 (2016) pp. 1923-1928.
- [12] Habte, L., Shiferaw, N., Mulatu, D., Thenepalli, T., Chilakala, R., & Ahn, J. W. Synthesis of nano-calcium oxide from waste eggshell by sol-gel method. *Sustainability*, vol 11, issue 11 (2019) p. 3196.
- [13] Daulay, A., & Gea, S. Extraction silica from rice husk with NaOH leaching agent with temperature variation burning rice husk. *Rasayan Journal of chemistry*, vol 14, issue 3 (2021).
- [14] Bakdash, R. S., Aljundi, I. H., Basheer, C., & Abdulazeez, I. Rice husk derived Aminated Silica for the efficient adsorption of different gases. *Scientific reports*, vol 10, issue 1 (2020) p. 19526.
- [15] Shamsudin, R., Ismail, H., & Hamid, M. A. A. The suitability of rice straw ash as a precursor for synthesizing β -wollastonite. In *Materials Science Forum*, vol 846, (2016) pp. 216-222. Trans Tech Publications Ltd.
- [16] Abd Rashid, R., Shamsudin, R., Hamid, M. A. A., & Jalar, A. In-vitro bioactivity of wollastonite materials derived from limestone and silica sand. *Ceramics International*, vol 40, issue 5 (2014) pp. 6847-6853.
- [17] Andalia, R., RAHMI, R., JULINAWATI, J., & Helwati, H. Isolation and characterization of cellulose from rice husk waste and sawdust with chemical method. *Jurnal natural*, vol 20, issue 1 (2020) pp. 6-9.
- [18] Radenahmad, N., Reza, M. S., Bakar, M. S. A., & Azad, A. K. Thermochemical characterization of rice husk (*Oryza sativa* Linn) for power generation. *ASEAN Journal of Chemical Engineering*, vol 20, issue 2 (2020) pp. 184-195.
- [19] Obeid, M. M.. Crystallization of synthetic wollastonite prepared from local raw materials. *Int. J. Mater. Chem*, vol 4, issue 4 (2014) pp. 79-87.

Conflict of interest statement: The author declares no conflict of interest.

Author contributions statement: Conceptualization, Nur Hasnidah, and Syed Nuzul Fadzli; Methodology, Nur Hasnidah; Formal Analysis, Nur Hasnidah; Investigation, Nur Hasnidah; Resources, Syed Nuzul Fadzli; Data Curation, Nur Hasnidah; Writing – Original Draft Preparation, Nur Hasnidah; Writing – Review & Editing, Syed Nuzul Fadzli; Visualization, Nur Hasnidah; Supervision, Syed Nuzul Fadzli.